Geophysical Prospecting of Parts of Isara-Remo, Ogun State, southwestern Nigeria Using 2D Electrical Resistivity Tomography

Olukayode D. Akinyemi
Federal University of Agriculture Abeokuta
Biodun S. Badmus
Federal University of Agriculture Abeokuta
Godwin A. Ajiboye
Federal University of Agriculture Abeokuta
Adebukonla O. Adeyemi (adekanmbiadebukonla@gmail.com)
Federal University of Agriculture Abeokuta
Moyosoluwa O. Adeyemi
Crawford University

Research Article

Keywords: Isara-Remo, Dipole-Dipole, Groundwater, Sedimentary-basement contact

Posted Date: November 11th, 2022

DOI: https://doi.org/10.21203/rs.3.rs-2248308/v1

Abstract

Geophysical survey using 2D Electrical Resistivity Tomography was conducted at Isara-Remo to delineate the sedimentary/basement contact as well as to prospect for the groundwater resources. Ten profiles were investigated using the Dipole-dipole array configuration and the resistivity data were processed and inverted using AGI Earth Imager software. The models obtained revealed the lithological composition of the area characterized generally by topsoil, sand, laterite, saturated sandy clay, dry sandy clay, dry clay, saturated clay, sandy clay, clayey sand, sandstones, coarse sand, shale, quartzite rock and basement rock. The models of the studied areas revealed resistivity ranges of 20.4 Ωm – 1832 Ωm; 11.6 Ωm – 327 Ωm; 6.4 Ωm – 2954 Ωm; 1.9 Ωm – 2767 Ωm; 25.7 Ωm – 1607 Ωm; 51.6 Ωm – 929 Ωm; 35.7 Ωm – 2659 Ωm; 42.5 Ωm – 1562 Ωm; 49.4 Ωm – 6113 Ωm; and 82 Ωm – 6783 Ωm for profile 01, 02, 03, 04, 05, 06, 07, 08, 09 and 10 respectively with corresponding depths of investigation at 174m, 78m, 197m, 174m, 105m, 174m, 197m, 105m, 99m and 99m. The study revealed the hydrogeological characterization and aquifer configuration of Isara, Profile 02 in ward 1 had the best groundwater potential due to its resistivity value in comparison to Profile 10 in ward 4 with low water-bearing aquifer. The qualitative information and to an extent, quantitative information on the groundwater potential in the study area have been provided and the sedimentary region delineated from the basement zones.

1 Introduction

Examining the earth's interior involves applying physical principles to study the earth's composition and environmental influence on it. Geophysical investigations act as a primary tool in almost all hydrological studies in visualizing the subsurface through the response of measurable physical parameters integrated with the site's geological inference (Andrade, 2011). These investigations assist the engineers in solving problems through the detection of different physical properties of the soil by sending a physical property and receiving it again (Hameda, 2013). These physical properties are measured using different geophysical methods which include the electrical method, gravity method, magnetic method, seismic method and induced polarization method. One of the most commonly applied techniques of geophysical surveying is electrical resistivity tomography (ERT) which measures the electrical resistance of the soil (Hameda, 2013) and this technique has been applied to this study.

Geophysical prospecting is usually conducted to locate probable positions of economically significant accumulations of oil, natural gas, groundwater and other minerals deposits. In subsurface investigations, the resistivity of the underlying materials depends on properties such as water content (which help in getting information about groundwater levels), aquifer boundaries, porosity and mineral contents.

In groundwater studies, several geophysical methods have been deployed but the electrical method has shown a wider approach and better applicability in groundwater science. It has been used worldwide for the delineation of groundwater resources in complex hydrogeological set-ups and had been studied by many researchers viz: Owen et al., 2005; Adepelumi et al., 2006; Daily et al., 2004; Kumar et al., 2010; Robert et al., 2011; Kumar *et al.*, 2012; Krishnamurthy et al., 2000; Butayneh, 2001; Kumar, 2004; Rao et

al., 2008; Kumar et al., 2008; Kumar et al., 2011; Ratnakumari et al., 2012; Revil et al., 2012; Abdulaziz et al., 2012; Hamzah et al., 2006; Osazuwa and Chii, 2010; Abdullahi and Osazuwa, 2011; Kadri and Nawawi, 2010; Anthony and John, 2010; Dutta et al., 2006; Rai et al., 2013.

Electrical resistivity tomography (ERT) is a technique where the resistivity changes in the vertical direction, as well as the horizontal direction along the survey line, are imaged in either two-dimensional or three-dimensional models (Hameda, 2013). The interpreted 2D inverted resistivity models of the subsurface is a pseudo-section plot that gives a simultaneous display of both horizontal and vertical variations in resistivity which represents hydrogeological conditions, structural features, and resistive and conductive formations of the area.

Resistivity surveys give a picture of the material resistivity distribution. Basically, it gives us information on electric resistivity properties of analysed material towards passing electrical current (Lazzari *et al*., 2006, Sass et al., 2008). Electrical methods of geophysical investigations are based on the resistivity (or its inverse, conductivity) contrasts of the subsurface materials which is described by Ohm's law.

The electrical resistance of the body $R\,(\Omega)$ is defined by the Ohm's law as follows:

$$R = \frac{V}{I}$$

Where V being the potential(v)

I is the current (A)

Ohm's law relates the voltage of a circuit to the product of the current and the resistance

The electrical resistance R, of a material is related to its physical dimension, cross sectional area A, and length l through the resistivity ρ, or its inverse, conductivity σ, by

$$\rho = \frac{1}{\sigma} = \frac{RA}{l}$$

Where R is the electrical resistance (Ω), l is the length of the cylinder (m), A is the cross-sectional area $\left(m^2\right)$

Artificially generated electric current are supplied to the soil and the resulting potential differences were measured.

2. The Study Area

Isara-Remo is the largest town in Remo North local Government Area of Ogun State. The area falls between latitudes 6˚58.5 N and 7˚0N and longitudes 3˚40E and 3˚42.5 E and from its southern and western boundaries, it stretches for about 30 kilometers northward and eastward.

It is situated about 80 kilometers from the commercial nerve center of the country, Lagos and has approximately 50 kilometers bearing from Ibadan and 70 kilometers bearing of Abeokuta, the state capital. Isara-Remo lies partially within the basement complex of South Western Nigeria and transits largely into sediments of the Dahomey basin. The study area has a tropical wet and dry climate characterised by heavy annual rainfall, high temperature and relative humidity. The area is a transitional zone with highly weathered basement rocks. The sedimentary rock in the area is composed of reddish sand stone i.e. the Oolitic iron stone and alluvium deposit indicative of Abeokuta Formation. Isara-Remo is well known for its high and rocky terrains and its geology which comprises of basement complex, sedimentary terrain and transition zones sometimes makes it difficult to study the subsurface models, archaeological features and proper information on the level and quantity of groundwater at discrete locations. Exploration and exploitation of resources in hard rock terrain is a challenging task because rocks exhibit inherent heterogeneity. According to Ariyo and Adeyemi (2011), secondary features developed in hard rocks such as faults, fractures, lineament and dykes control the groundwater flow and movement. These features are as a result of the heterogeneity of the rock underlying the area. Hence, this characteristics of rocks have arisen an interest to reveal geoelectrically, the geological formations and subsurface images of the cross sections of the bearing soil with complex layers and structures for industry and groundwater resources within Isara-Remo. Using 2-Dimesional Electrical Resistivity Tomography (ERT) in Isara-Remo has the potential of revealing the overburden thickness, lithological variations within the crust, and aquifer characteristics for groundwater reserves and distribution.

3. Methodology

3.1 Data Acquisition Method

Survey sites were selected across the 4 wards in the study area for easy data distribution within the town. In ward 1, three sites were selected which include profiles 01, 02 and 05. In ward 2, two sites were selected, which includes profiles 03 and 04. While in ward 3, three sites were also selected, which includes profiles 06, 07 and 08. For ward 4, two sites were selected which includes profiles 09 and 10. 2D ERT was carried out at all 10 profiles using the AGI Super Sting R8 IP Terrameter and the Dipole-dipole array configuration was applied. The data inversion was carried out using the AGI Earth Imager 2D inversion software designed for the equipment. The base map of the study area indicating the profile locations is as shown in Fig. 1.

4. Results And Discussion

The results of the data obtained using 2D ERT were analysed with the EarthImager 2D Software and they vary from profile to profile outlined in the sections below.

4.1 Ward 1

Profile 01 is located at coordinate N 6°58’60.723, E 3°41’13.7405 to N 6°59’00.104, E 3°41’52.8400 with a profile length of $840m$ (Fig. 3). From the inverted resistivity section, it was evident from the section that the geological formations for this profile were characterised with measured resistivity values that ranged from $20.4\Omega m$ to $1832\Omega m$ within a depth of $174m$. The result from the ERT suggested a geological environment with lateral differences along the survey lines. The resistivity model indicated the presence of sand in the topsoil and this occupied a depth of $25m$, except a small zone of aquifer between lateral distance $610m$ and $680m$. This portion is actually close to a stream around that location. Below this layer comprise a body of lateritic soil with resistivity ranging from $500\Omega m$ to $1800\Omega m$ extending eastwards from a depth of $10m$ downwards between $440m$ to $780m$. A low resistivity anomaly occurred below lateral distance of $340m$ at a depth of $26m$ extending to $150m$ indicating huge potentiality of groundwater and it is a huge aquifer as depicted in the resistivity section. The resistivity of this aquifer zone varies from $27.8\Omega m$ to $100.0\Omega m$ representing the deposition of clay saturated with water. This is a potential site for exploitation of the groundwater resource at deeper depth for long term sustainability of the aquifer system in the area. On the eastern side, the high resistivity body ($500\Omega m$ to $1800\Omega m$) is completely massive and devoid of groundwater between lateral distance of $440m$ to $790m$.

Profile 02 is situated at coordinate N 6°59’05.571, E 3°40’54.3604 to N 6°58’50.893, E 3°40’48.7011 with a length of $498m$ using $6m$ electrode spacing and a total of 84 electrodes. A depth of $78m$ was investigated and the resistivity section ranged from $11.6\Omega m$ to $327\Omega m$ as shown in Fig. 3. The resistivity model indicated the presence of topsoil and sand with resistivity values that ranged from $53.7\Omega m$ to $287.6\Omega m$ within a depth of $12m$. Below this section, was a low resistivity zone which ranged from $11.6\Omega m$ to $35\Omega m$ and occured between $15m$ and $40m$ depth. This lateral layer extended from the north to the south of this profile. This zone is inferred as the water bearing horizon at a shallow depth which is suspected to be of low yield. Profile 02 depicts three horizontal layers with topsoil layer of $10m$ thickness and sand formation ($53.7\Omega m - 287.6\Omega m$). This layer is underlain by a thick layer of weathered/ moderately weathered formation ($11.6\Omega m$ to $35\Omega m$) laterally and is extended up to $40m$ depth. The second layer occupied the depth between $8m$ and $40m$ and had resistivity that ranged from $\tilde{1}1\Omega m$ to $35\Omega m$. It consisted of saturated clay and was regarded as the most favourable zone for groundwater exploration within the site. The third resistivity zone represents a body of saturated sandy clay and shows higher resistivity values ranging from $50\Omega m$ to $82\Omega m$ when compared to the second layer.

Profile 05 is situated at coordinate N 6°58’54.424, E 3°41’24.0664 and N 6°59’10.295, E 3°41’15.1925 having a profile length of $664m$ and electrode spacing of $8m$ (Fig. 3). A total depth of $105m$ was investigated and the inverted resistivity section ranged from $25.7\Omega m$ to $1607\Omega m$. The model shows a surface layer of low to moderately high resistivity with the northern region dominated by high resistivity values that ranged from $615\Omega m$ to $1600\Omega m$ and this was interpreted as lateritic topsoil. The mid to southern region shows a distribution of similar materials at the surface with lower resistivity values that ranged from $400\Omega m$ to $600\Omega m$ sparsely distributed. Other materials with lower range of resistivity

values $(80\Omega m - 200\Omega m)$ representing dry sandy clay occupied a large portion of the profile ($0 - 450m$) down to an average vertical distance of $6m$. Saturated clay with resistivity values that ranged from $26\Omega m$ to $105\Omega m$ occupied a greater portion beneath the surface layer and was interpreted to be a zone with high groundwater potential. This zone has a thickness of $10m$ which increased vertically to $65m$ between lateral distance of $213m$ and $600m$. Other than this region, the remaining part of the profile comprised of moderate resistivity layer with resistivity value that ranged from $180\Omega m$ to $500\Omega m$ and was classified as clayey sand occupying a greater portion of the section.

4.2 Ward 2

Profile 03 is situated at coordinate N 6°59'14.701, E 3°40'46.0956 and N 6°59'04.122, E 3°40'20.1059 with profile length of $840m$ using $10m$ electrode spacing. A total depth of $197m$ was investigated and the resistivity ranged from $6.4\Omega m$ to $2954\Omega m$ as depicted in Fig. 4. The model indicated a contrasting resistivity body at the top layer. The top layer had resistivity that ranged from $47.0\Omega m$ to $3361\Omega m$ and extended from the surface to a depth of $5m$ within the profile. Between lateral distances of $590m$ to $840m$, the resistivity was high and greater than $500\Omega m$ and this zone was considered to be devoid of groundwater. At lateral distance between $370m$ and $380m$, the resistivity was low $44\Omega m$; an indication of groundwater potential. The other resistivity values $> 200\Omega m$ suggested the composition of sandy clay within that zone. Beneath the topsoil, there was evidence of water saturation in small patches occurring between lateral distance $100m$ and $570m$ at a depth between $5m$ and $47m$ and had resistivity values that ranged from $6.4\Omega m$ to $70\Omega m$. This zone is suspected to be of low yield aquiferous zone. Below the second zone, there was no potential groundwater prospect as this region seems to be composed of dry clayey sand.

Profile 04 is situated at coordinates N 6°59'23.344, E 3°40'36.6894 to N 6°59'20.027, E 3°40'10.4492; parallel to profile 03. The profile length was $840m$ with $10m$ electrode spacing (Fig. 4). The depth of investigation was $174m$ and the values of the resistivity ranged from $1.9\Omega m$ to $2767\Omega m$. The inverted model revealed the topsoil layer which comprised of laterite mostly and resistivity that ranged from $570\Omega m$ to $2315\Omega m$ between a distance of $350m$ to $840m$.

There was a progressive increase in the depth of the lateritic soil from a depth of about $5m$ at a lateral distance of $330m$ to a depth of $87m$ at a lateral distance of $840m$. There was a saturated clay region from lateral distance of $330m$ to $570m$ at a depth between $20m$ and $60m$ with resistivity values that ranged from $17\Omega m$ to $40\Omega m$. This region depicts a low yield aquiferous zone. Also, on the eastern part, there was a presence of clayey sand, indicated by low resistivity that ranged from $200\Omega m$ to $400\Omega m$ and dry sandy clay comprised the region below the saturated clay region.

4.3 Ward 3

Profile 06 is situated at coordinates with a profile length of $840m$ using $10m$ electrode spacing (Fig. 5). A depth of $174m$ was investigated and the resistivity values ranged from $51.6\Omega m$ to $929\Omega m$. From the inverted resistivity model, a surface layer of moderately high resistivity body $(230\Omega m$ to $920\Omega m)$ was revealed from the surface to a depth of $15m$. Between lateral distances of $310m$ to $380m$, a low

resistivity zone $(110\Omega m - 150\Omega m)$ was present, and this suggested a water body close to this region. This zone appeared to be the recharge site of an aquifer body which occupied the west side of the profile. This aquifer is favourable for groundwater exploration as it occupies to a depth of $13m$ to $126m$ and could be a prospective borehole location. Other than this region, smaller prospective groundwater zones appear in patches centrally between lateral distance of $441m$ and $469m$ with a thickness of $16m$, at a distance of $553m$ to $575m$ with a thickness of $20m$ and towards the eastern part of the profile between $730m$ to $774m$ at a depth of $22m$ to $51m$. Other regions in this profile comprise moderate of high resistivity value $(> 200\Omega m)$ interpreted as dry sandy clay and compacted sandstone.

Profile 07 is situated at coordinate N 6°59'29.381, E 3°41'12.8413 to N 6°59'54.973, E 3°41'14.2475 perpendicular to profile 06. The profile length was $840m$ using an electrode spacing of $10m$ and a depth of $170m$ was investigated while the resistivity ranged from $35.7\Omega m$ to $2659\Omega m$ (Fig. 5). The resistivity layer indicates the presence of a three-layer model represented by the 2D section. The first layer comprises of the lateritic topsoil and sand formation with resistivity that ranged from $200\Omega m$ to $2659\Omega m$ from the surface to a depth of $25m$. This layer is immediately underlain by a low to high saturated layer with resistivity that ranged from $37\Omega m$ to $190\Omega m$ and a thickness of about $50m$ average. This layer is favourable for groundwater exploration within the area. The third layer represented a body of sandstone, clayey sand and sandy clay having moderate resistivity values that ranged from $240\Omega m$ to $650\Omega m$.

Profile 08 is situated at coordinates N 6°59'52.164, E 3°40'58.0130 to N 6°59'49.440, E 3°41'12.6751 parallel to profile 06 and the profile length was $498m$. A depth of $105m$ was investigated and the resistivity ranged from $42.5\Omega m$ to $1562\Omega m$ (Fig. 5).

The resistivity model revealed a contrasting resistivity body at the top layer. It ranges from $82\Omega m$ to $127\Omega m$ at a distance of $214m$ to $252m$, $450\Omega m$ to $1200\Omega m$ at lateral distance of $374m$ to $495m$ and $170\Omega m$ to $300\Omega m$ interspersed between the first two resistivity zones. Beneath the top layer, from a depth of $5m$ to $38m$ on the western part, a low resistivity body ($42.5\Omega m$ to $91\Omega m$) which suggested the presence of groundwater table within the area was observed. It suggested the possibility of high yielding hand dug wells extending from lateral distance of $0m$ to $200m$. Also, between lateral distance of $330m$ to $418m$, a saturated body was also identified from a depth of $18m$ downwards. This suggested huge potentiality of groundwater and this site appears to be favourable for borehole drilling within the region. The other regions within the model seem to be comprised of sandy clay.

Ward 4

Profile 09 is situated at coordinates N 7°00'00.625, E 3°41'01.9037 to N 7°00'12.174, E 3°41'08.9277. and a profile length of $415m$ was investigated using $5m$ electrode spacing. The depth of investigation was $99m$ and the resistivity section ranged from $49.4\Omega m$ to $6113\Omega m$ (Fig. 6). From the inverted resistivity model, a surface layer of moderately high resistivity body ($100\Omega m$ to $1000\Omega m$) was revealed except at lateral distance of $348m$ to $360m$ where the resistivity value was very high ($2998.2\Omega m$ to $6113.2\Omega m$) and indicated the presence of basement rock and coarse sand to a depth of $10m$. Between lateral

distance of $304m$ and $345m$, the resistivity was lowest ($49.4\Omega m$ to $82\Omega m$) and occurred at a depth of $11m$ to $31m$. This zone appeared to be the only favorable zone for groundwater exploration within the area. At lateral distances from $38m$ to $208m$, the resistivity was relatively high ($1000\Omega m$ to $4105\Omega m$) and revealed the occurrence of sand stone and quartzite rock within the depth of $8m$ to $41m$. This zone also appeared between lateral distance of $374m$ to $400m$ at a depth of $5m$. Other regions had moderately resistivity values ($300\Omega m - 620\Omega m$) which can be interpreted as shale/dry sandy clay.

Profile 10 is situated at coordinate N 7°00'03.079, E 3°40'53.5964 and N 7°00'05.049, E 3°41'05.0389 perpendicular to profile 09. The profile length was $415m$ and electrode spacing of $5m$ was used. A depth of $99m$ was investigated and the resistivity section ranged from $82\Omega m$ to $6783\Omega m$ (Fig. 6). The model revealed the presence of topsoil and sand with resistivity that ranged from $82.3\Omega m$ to $1150\Omega m$ within a depth of $6m$. Below this layer, between lateral distance of $18m$ and $317m$, a large high resistivity body occurred ($1000\Omega m$ to $6782\Omega m$), and this suggested the presence of massive quartzite rock from a depth of $9m$ to the end of the profile. Other region within the profile revealed moderate resistivity ($600\Omega m$ to $1000\Omega m$) which indicated the presence of compacted sandstone. From the inverted resistivity section, there was no groundwater prospective zone within the profile.

DISCUSSION

The study revealed the lithological composition of the subsurface within of the study area. It revealed resistivity values ranging from $20.4\Omega m$ to $1832\Omega m$; $11.6\Omega m$ to $327\Omega m$ and $25.7\Omega m$ to $1607\Omega m$ for profile 01, profile 02 and profile 05 at depths of $174m$, $78m$ and $105m$ respectively in Ward 1. The geoelectric model composed of laterite, sand, saturated clay, sandy clay, and clayey sand. Profile 02 had the lowest resistivity values recorded within the town. Due to the low resistivities observed, this location has the highest groundwater prospect. The results obtained in this region were similar to the results obtained at Ode-Remo in the study by Ariyo and Adeyemi in 2012 and this region can be depicted as a sedimentary zone.

Ward 2 revealed the resistivity values to range from $6.4\Omega m$ to $2954\Omega m$ and $1.9\Omega m$ to $2767\Omega m$ for profiles 03 and 04 to a depth of $197m$ and $174m$ respectively. The lithology within the region compose of laterite, sandy clay, clayey sand and dry sandy clay and saturated clay deposits within the area. Profiles 03 and 04 are parallel to each other and revealed similar model composition. The region had weak/ poor groundwater potentials where available and only to a depth of about $50m$. The groundwater potential in this region is low due to the high resistivities. The lithology of this region was inconclusive from the resistivity result and aquifer potential obtained in this study.

For Ward 3 profiles 06, 07 and 08 have the resistivity value to range from $51.6\Omega m$ to $929\Omega m$, $35.7\Omega m$ to $2659\Omega m$ and $42.5\Omega m$ to $1562\Omega m$ and the geoelectric model revealed the composition of laterite, sandy clay, clayey sand, sandstones, compacted sandstones and saturated clay up to depths of $174m$, $197m$ and $105m$. Profile 08 revealed the best groundwater potential in the ward. The results obtained in the region and the moderately low resistivity values recorded depicted the region as a sedimentary terrain.

For Ward 4, the resistivity model ranges from $49.4\Omega m$ to $6113\Omega m$ and $82\Omega m$ to $6783\Omega m$ for profiles 09 and 10 respectively and their depths of investigation were $99m$. The geological model layer of the region revealed the presence of shale, dry clay, clayey sand, sandy clay, coarse sand, sandstone, compacted sandstone, quartzite rock, basement rock and fractured basement. Profile 09 had the lowest groundwater prospective zone while at Profile 10, there was no noticeable confined aquifer structure. The results obtained in this ward were similar to the results obtained in the adjourning town as reported in the study by Ariyo and Adeyemi (2009) conducted in Fidiwo and Ajebo. Due to the composition of the studied region and the geology of the adjourning towns, it could be concluded that the ward was a basement complex region.

Conclusion

The resistivity models suggest that the lithology of the studied region is diverse and the study has revealed that the locations studied have a subsurface geological characteristics composed mainly of laterite, dry sand, shale, saturated clay, dry clay, sandy clay, clayey sand, sandstone, compacted sandstone, quartzite rock, basement rock, fractured basement to a depth of about 150m. The study has also revealed the hydrogeological characterization and aquifer characteristics of Isara-Remo as well as the potential zones for aquifers. The northern part of the town (i.e. Ward 4) has weak groundwater prospect as the two profiles 09 and 10 revealed that there was no promising confined aquifer structures *N - S/E - W*. This region occupied Abeokuta formation and the zone belongs to the Abeokuta group as concluded by Ariyo *et al.* (2009). On the Eastern part of the town where profiles 06, 07 and 08 were investigated, the groundwater aquifer zone is suspected to be decreasing eastward along the profiles 06 & 08 and also, the groundwater potential increases towards the south. Also, on the western part of the town where profiles 03 & 04 were investigated, the groundwater zones present were generally weak. And on the southern part of the town, profile 02 revealed a lateral groundwater level north to south of the profile, while profile 01 revealed only a region of groundwater potential northwards and profile 05 revealed only a small compacted groundwater potential zone centrally. In this study, data from the geophysical investigation using ERT has provided qualitative information on the groundwater resources of Isara-Remo and more geophysical investigations is hereby recommended in wards 2, 3 and 4 to properly delineate the transition zones within the town.

References

1. Abdulaziz, A.M., Hurtado, J.M. and Faid, A. (2012) Hydrogeological Characterization of Gold Valley: An Investigation of Precipitation Recharge in an Intermountain Basin in the Death Valley Region, California, USA, Hydrogeology Journal, Vol. 20, No. 4, 701–718.
2. Abdullahi, N.K. and Osazuwa, I.B. (2011) Geophysical Imaging of Municipal Solid Waste Contaminant Pathways. Environ. Earth Sci., 62, 1173–1181.
3. Adepelumi, A.A., Yi, M.J., Kim, J.H., Ako, B.D. and Son, J.S. (2006) Integration of Surface Geophysical Methods for Fracture Detection in Crystalline Bedrocks of Southwestern Nigeria, Hydrogeology

Journal, Vol. 14, 1284–1306.

4. Ahzegbobor Philips Aizebeokhai (2010) 2D and 3D Geoelectrical Resistivity Imaging: Theory and Field Design. Scientific Research and Essays, vol. 5(23), pp 3592–3605.
5. Andrade R. (2011) Intervention of Electrical Resistance Tomography (ERT) in Resolving Hydrological Problems of a Semi-Arid Granite Terrain of Southern India. Journal of Geological Society of India, Vol. 78, pp. 337–344.
6. Anthony, A.A. and John, R.O. (2010) 2D Electrical Imaging and its Application in Groundwater Exploration in Part of Kubanni River Basin, Zaria, Nigeria. World Rural Obs., 2(2), 72–82.
7. Ariyo, S.O., Adeyemi, G.O., Oyebamiji, A.O. (2009) Electromagnetic VLF Survey for Groundwater Development in a Contact Terrain; A Case Study of Ishara-Remo, Southwestern Nigeria. Journal of Applied Sciences Research, 5(9): 1239–1246.
8. Ariyo, S. O. and Adeyemi, G. O. (2009) Role of Electrical Resistivity Method for Groundwater Exploration in Hard Rock Areas: A Case Study from Fidiwo/Ajebo Areas of Southwestern Nigeria. The Pacific Journal of Science and Technology, Volume 10, Number 1, pp 483–486.
9. Ariyo, S.O. and Adeyemi, G.O. (2011) Integrated Geophysical Approach for Groundwater Exploration in Hard Rock Terrain. A Case Study from Akaka Area of Southwestern Nigeria. International Journal of Advanced Scientific and Technical Research, Issue 1, Volume 2, pp 376–395.
10. Ariyo, S.O. and Adeyemi, G.O. (2012) Geoelectrical Characterization of Aquifers in the Basement Complex/ Sedimentary Transition Zone, Southwestern Nigeria. International Journal of Advanced Scientific Research and Technology, Issue 2, Volume 1, pp 43–54.
11. Badmus, G.O., Akinyemi, O.D., Gbadebo, A.M. et al. (2021) Assessment of seasonal variation of saltwater intrusion using integrated geophysical and hydrochemical methods in some selected part of Ogun Waterside, Southwest, Nigeria. Environ Earth Sci 80, 99. https://doi.org/10.1007/s12665-021-09379-y
12. Batayneh, Awni T. (2001) Resistivity Imaging for Near-Surface Resistive Dyke Using Two-Dimensional DC Resistivity Techniques, Journal of Applied Geophysics, Vol. 48, pp. 25–32.
13. Bhattacharya, P.K. and Patra, H.P. (1968) Direct Current Geoelectric Sounding, Principles and Interpretation, Methods in Geochemistry and Geophysics, Series-9. Elsevier Publishing Company, 135 p.
14. Chambers, J.E., Ogilvy, R.D., Kuras, O., Cripps, J.C. and Meldrum, P.I. (2002) 3D Electrical Imaging of Known Targets at a Controlled Environmental Geology, 41, 690–704.
15. Chambers, J.E., Wilkinson, P.B., Weller, A.L., Kuras, O., Meldrum, P.I., Ogilvy, R.D., Aumonier, J., Penn, S., Wardrop, D.R., Bailey, E., Joel, P. and Griffiths, N. (2009) Sand and Gravel Deposit Evaluation using Electrical Resistivity Tomography. Near Surface Geoscience- 15th European meeting of Environmental and Engineering Geophysics, Dublin, Ireland.
16. Chambers, J.E., Wilkinson, P.B., Weller, A., Meldrum, P.I., Kuras, O., Ogilvy, R.D., Aumonier, J., Bailey, E., Griffiths, N., Matthews, B., Penn, S. and Wardrop, D. (2011) Characterizing Sand and Gravel Deposits using Electrical Resistivity Tomography (ERT): Case Histories from England and Wales. Pp. 166–172

in Hunger, E. and Walton, G. (Eds.). Proceedings of the 16th Extractive Industry Geology Conference, EIG Conferences Ltd.

17. Christensen, N. B. and Sorensen, K. I. (1994) Integrated Use of Electromagnetic Methods For Hydrogeological Investigations. Proceedings of the Symposium on the Application of Geophysics to Engineering and Environmental Problems, March 1994, Boston, Massachusetts, pp 163–176.
18. Dahlin, T. (1996) 2D Resistivity Surveying for Environmental and Engineering Applications. First Break, vol. 14, pp. 275–284.
19. Dahlin, T. and Owen R. (1998) Geophysical Investigations of Alluvial Aquifers in Zimbabwe. Proceedings of the IV Meeting of the Environmental and Engineering Geophysical Society (European Section), Sept. 1998. Barcelona, Spain pp 151–154.
20. Daily, W., Ramirez, A., Binley, A. and Labrecque, D. (2004) Electrical Resistance Tomography. The Leading Edge, 438–442.
21. Dutta, S., Krischnamurthy, N.S., Arora, T., Rao, V.A., Ahmed, S. and Baltassat, J.M., (2006) Localization of Water-Bearing Fractured Zones in a Hard Rock Area Using Integrated Geophysical Techniques in Andhra Pradesh. Hydrogeol. J., 14, 760–766.
22. Fadele, S. I., Jatau, B. S. and Goki, N. G. (2013) Subsurface Structural Characterization of Filatan Area A, Zaria – Kano Road, Using the 2D Electrical Resistivity Tomography. Journal of Earth Sciences and Geotechnical Engineering, vol. 3, no. 1, 73–83.
23. Giao, P.H., Chung, S.G., Kim, D.Y. and Tanaka, H. (2003) Electric Imaging and Laboratory Resistivity Testing for Geotechnical Investigation of Pusan Clay Deposits, Jour. Appld. Geophys., Vol.52, 157–175.
24. Griffiths D.H. and Barker R.D. (1993) Two-Dimensional Resistivity Imaging and Modeling in Areas of Complex Geology. Journal of Applied Geophysics 29, 211–226.
25. Griffiths, D.H. and Turnbull, J. (1985) A Multi-Electrode Array for Resistivity Surveying. First Break, vol. 3(7), pp. 16–20.
26. Hamzah, U., Yaacup, R., Samsudin, A.R. and Ayub, M.S. (2006) Electrical Imaging of the Groundwater Aquifer at Banting, Selangor, Malaysia. Environ. Geol., 2006, 49, 1156–1162.
27. Hilbich C., Marescot L., Hauck C., Loke M.H. and Mausbacher R. (2009) Applicability of Electrical Resistivity Tomography Monitoring to Coarse Blocky and Ice-rich Permafrost Landforms. Permafrost and Periglacial Processes 20(3): 269–284.
28. Kadri, M.D. and Nawawi, M.N.M. (2010) Groundwater Exploration Using 2D Resistivity Imaging in Pagoh, Johor, Malaysia. In AIP Conference Proceedings, 2010, vol. 1325(1), pp. 151–154.
29. Keller, G.V. and Frischknecht, F.C. (1966) Electrical Methods in Geophysical Prospecting. Pergamon Press Inc., Oxford.
30. Krishnamurthy, N.S., Kumar, D., Negi, B.C., Jain, S.C., Dhar, R.L. and Ahmed, S. (2000) Electrical Resistivity Investigation in Maheshwaram Watershed, A.P., India, Technical Report No. NGRI-2000-GW-287.

31. Kumar, D. (2004) Conceptualization and Optimal Data Requirement in Simulating Flow in Weathered-Fractured Aquifers for Groundwater Management, *Ph.D. Thesis*, Osmania University, Hyderabad, 213 pp.
32. Kumar, D. (2012) Efficacy of Electrical Resistivity Tomography Technique in Mapping Shallow Subsurface Anomaly, Journal of Geological Society of India, Springer Publication, Vol. 80, No.3, 304–307.
33. Kumar, D., Nabi Aadil, Chandra, S., Sreedevi, P.D., Khan Haris H., Dutta, S., Zaidi, F.K., Ali Sayed, Krishnamurthy, N.S. and Ahmed, S. (2008) Groundwater Exploration in Basaltic Formations at Ghatiya Watershed, Madhya Pradesh: An Integrated Study, Technical Report No. NGRI-2008- GW-632.
34. Kumar, D., Rai, S.N., Thiagarajan, S., Ratna Kumari, Y. and Bulliabai, M. (2011) Sensitivity Analysis of 2D Electrical Resistivity Data for Groundwater Exploration in Deccan Basalt Hard Rock Aquifers, Presented and Published in Abstract volume on 'Andhra Pradesh Science Congress – 2011" on Focal Theme Science for the Society held at Visakhapatnam during 14–16 November 2011, p-194.
35. Kumar D., Rao V.A., and Sarma V. S. (2012) Hydrogeological and Geophysical Study for Deeper Groundwater Resource in Quartzitic Hard Rock Ridge Region from 2D Resistivity Data. CSIR- National Geophysical Research Institute, Hyderabad – 500007, India.
36. Kumar, D., Rao, V.A., Nagaiah, E., Raju, P.K., Mallesh, D., Ahmeduddin, M. and Ahmed, S. (2010) Integrated Geophysical Study to Decipher Potential Groundwater and Zeolite-Bearing Zones in Deccan Traps. Research Article in Current Science Vol. 98, No.6, 803–814.
37. Kunetz G. (1966) Principles of Direct Current Resistivity Prospecting. Gebruder Borntraeger, Berlin, p. 103.
38. Kuras, O., Pritchard, J., Meldrum, P.I., Chambers, J.E., Wilkinson, P.B., Ogilvy, R.D. and Wealthall, G.P. (2008) Monitoring Hydraulic Processes with Automated Time-Lapse Electrical Resistivity Tomography (ALERT). Comptes Rendes Geosciences – Special Issue on Hydrogeophysics, 341, 868–885.
39. Lazarri M., Geraldi E., Lapenna V. and Loperte A. (2006) Natural Hazards vs Human Impact: An Integrated Methodological Approach in Geomorphological Risk Assessment on the Tursi Historical Site, Southern Italy. Landslides 3, 275–287.
40. Lytle, R. J., and Dines, K. A. (1978) An Impedance Camera: A System for Determining the Spatial Variation of Electrical Conductivity; Lawrence Livermore National Laboratory UCRL-52413.
41. Martinez-Lopez J., Rey J., Duenas J., Hidalgo C. and Benavente J. (2011) Electrical Tomography Applied to the Detection of Subsurface Cavities. Journal of Cave and Karst Studies, v. 75, no. 1, p. 28–37.
42. Meyer de Stadelholfen, C. (1991) Application de la geophysique aux recherches d'eau Ed. Lavoisier, Paris.
43. Nyquist, L. E., Bradley, J. C. and Davis, R. K. (1999) DC Resistivity Monitoring of Potassium Permanganate Injected to Oxide TCL in Suii. Jour. Environ. Engg. Geophys. v4, pp 135–148.

44. Osazuwa, I.B. and Chii, E.C. (2010) Two-dimensional Electrical Survey around the Periphery of an Artificial Lake in the Precambrian Basement Complex of Northern Nigeria. International Journal of Physical Science, 2010, 5(3), 238–245.
45. Owen, R.J., Gwavava, O. and Gwaze, P. (2005) Multi-Electrode Resistivity Survey for Groundwater Exploration in the Harare Greenstone Belt, Zimbabwe, Hydrogeology Journal, Vol., 14, 244–252.
46. Rai, S.N., Thaigarajan, S., Kumar, D., Dubey, K.M., Rai, P.K., Ramachandran, A. and Nithya, B., (2013). Electrical Resistivity Tomography for Groundwater Exploration in a Granitic Terrain in NGRI Campus. Current Science, Vol.105, No. 10
47. Rao, V. A., Kumar, D., Chandra, S., Nagaiah, E., Kumar, G. A., Ali, Syed and Ahmed, S., 2008. High Resolution Electrical Resistivity Tomography (HERT) Survey for Groundwater Exploration at APSP Campus, Dichpally, Nizamabad District, Andhra Pradesh, Technical Report No. NGRI-2008-GW-626
48. Ratnakumari, Y., Rai, S.N., Thiagarajan, S. and Kumar, D. (2012) 2D Electrical Resistivity Imaging for Delineation of Deeper Aquifers in Parts of Chandrabhaga River Basin, Nagpur District, Maharashtra, India, Current Science, Vol. 102, No.1, 61–69.
49. Revil, A., Karaoulis, M., Johnson, T. and Kemna, A. (2012) Review: Some Low Frequency Electrical Methods for Subsurface Characterization and Monitoring in Hydrogeology, Hydrogeology Journal, Vol.20, No.4, 617–658.
50. Ritz, M., Pariscot, J. C., Diour S., Beauvais, A. and Dione, E. (1999) Electrical Imaging of Lateritic Weathering Mantles over Granitic and Metamorphic Basement of Eastern Senegal, West Africa. Jour. Appld. Geophys., v41, pp 335–344.
51. Robert, T., Dassargues, A., Brouyère, S., Kaufmann, O., Hallet, V. and Nguyen, F. (2011) Assessing the Contribution of Electrical Resistivity Tomography (ERT) and Self Potential (SP) Methods for a Water Well Drilling Program in Fractured/Karstified Limestones, Journal of Applied Geophysics, Vol.75, 42–53.
52. Sass O., Bell R. and Glade T. (2008) Comparison of GPR, 2D-resistivity and Traditional Techniques for the Subsurface Exploration of the Oschningen Landslide, Swabian Alb (Germany). Geomorphology 93: 89–103.
53. Sayed Hameda (2013) Electrical Resistance Tomography (ERT) Subsurface Imaging for Non-Destructive Testing and Survey in Historical Buildings Preservation. Australian Journal of Basic and Applied Sciences, 7(1): 344–357.

Figures

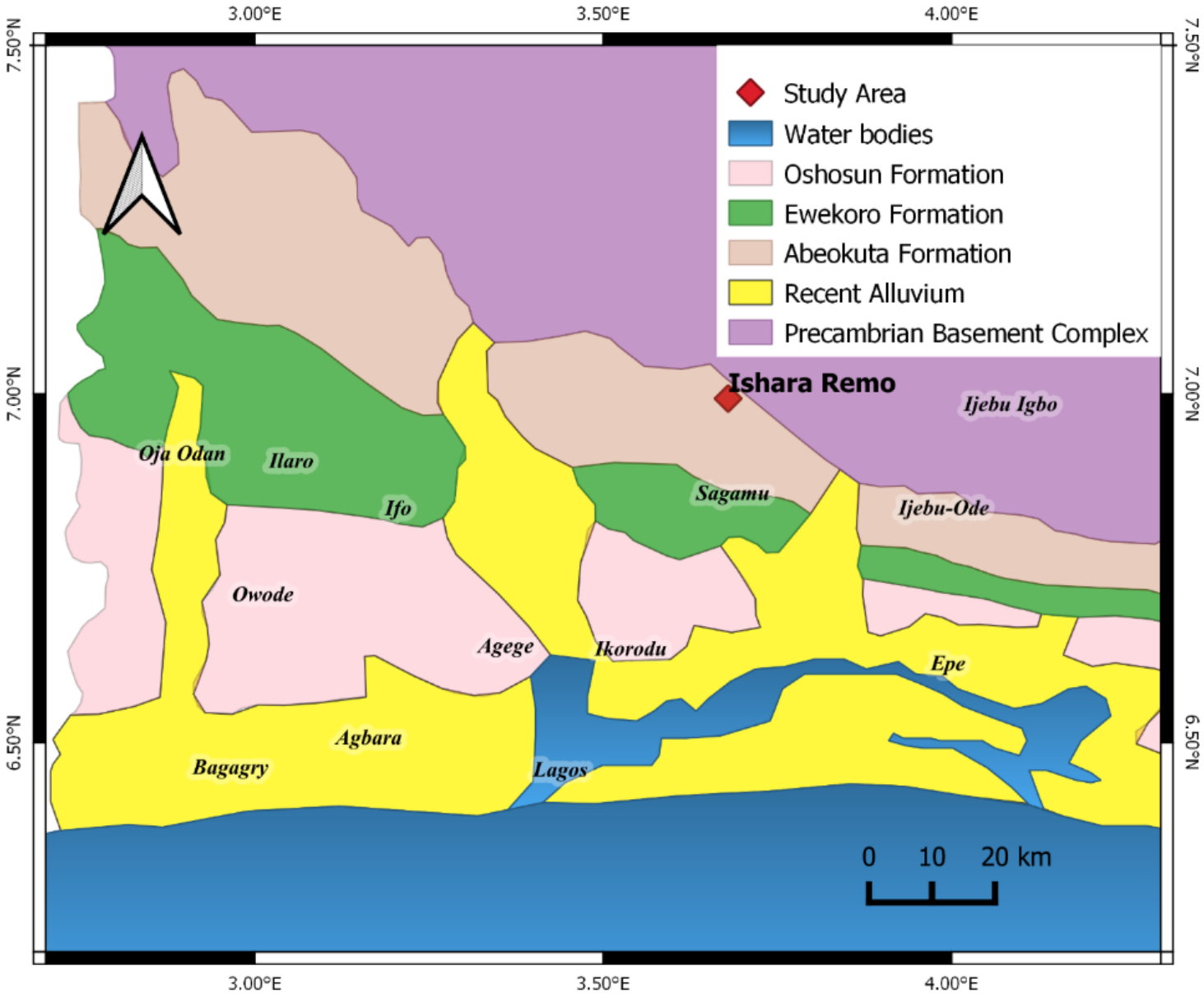

Figure 1

Geological map of eastern Dahomey Basin showing the study area

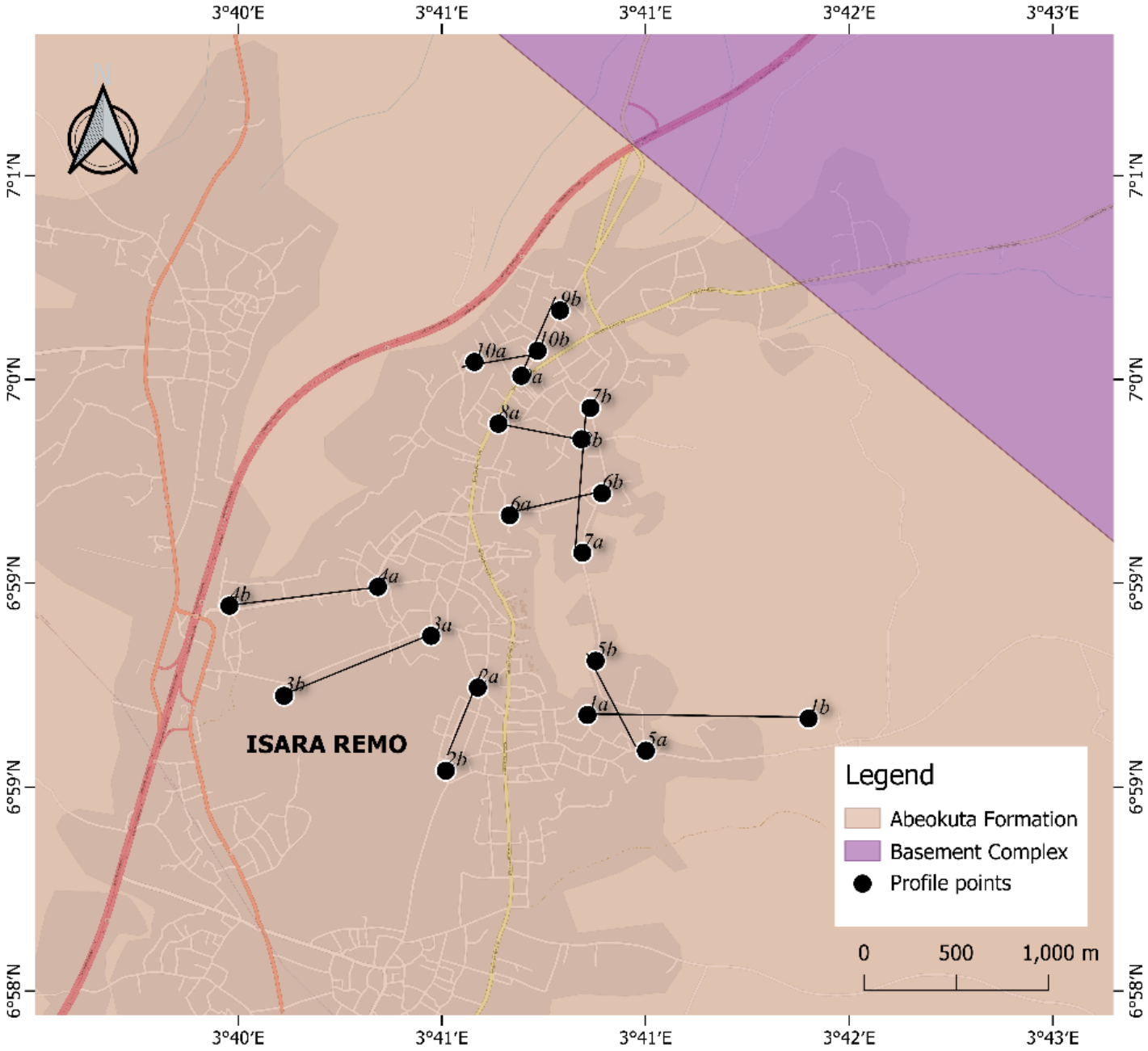

Figure 2

Geological map of Isara-Remo showing the Profile lines

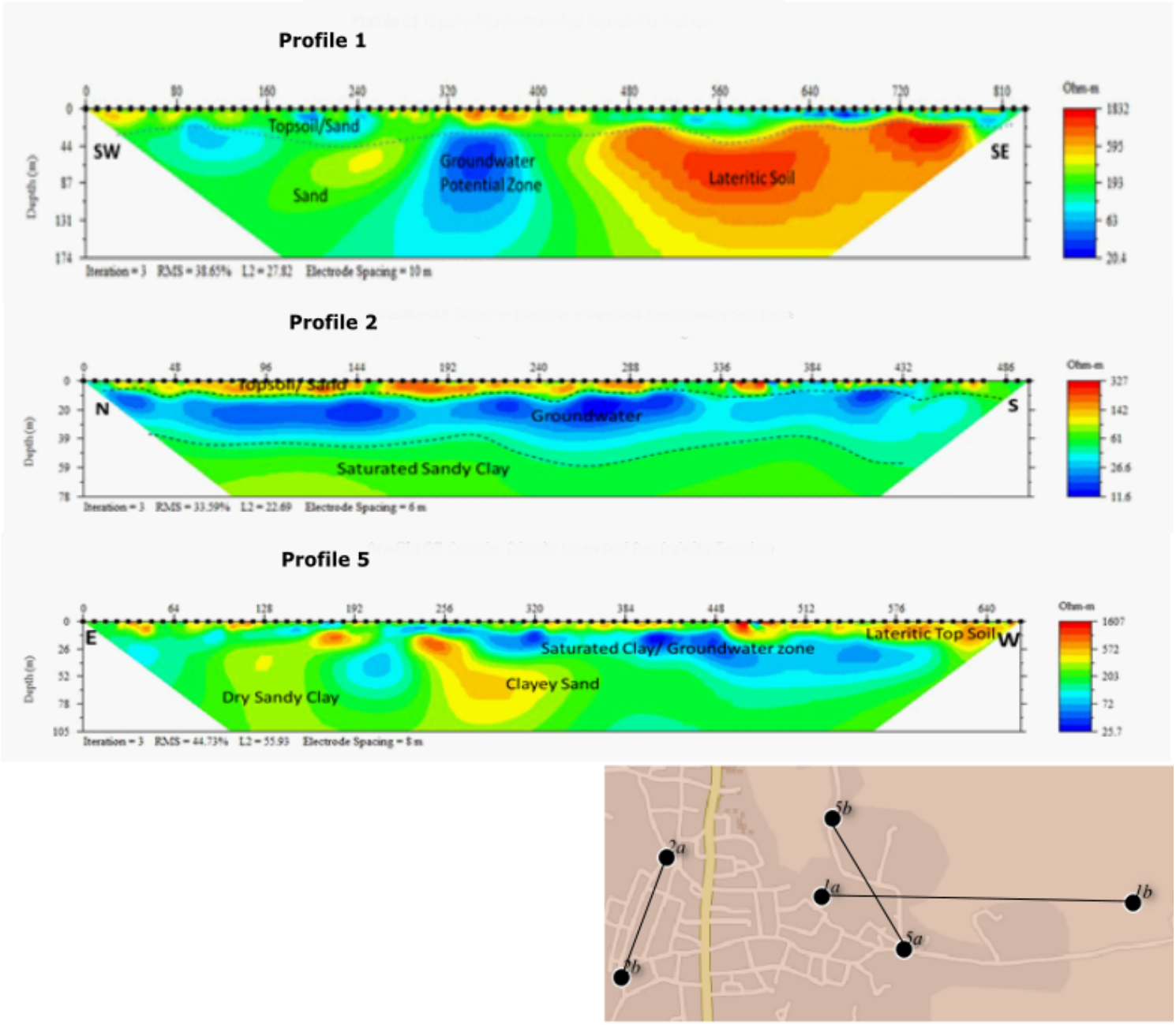

Figure 3

Dipole Dipole Inverted resistivity sections across Profile 1, 2 and 5 in Ward 1

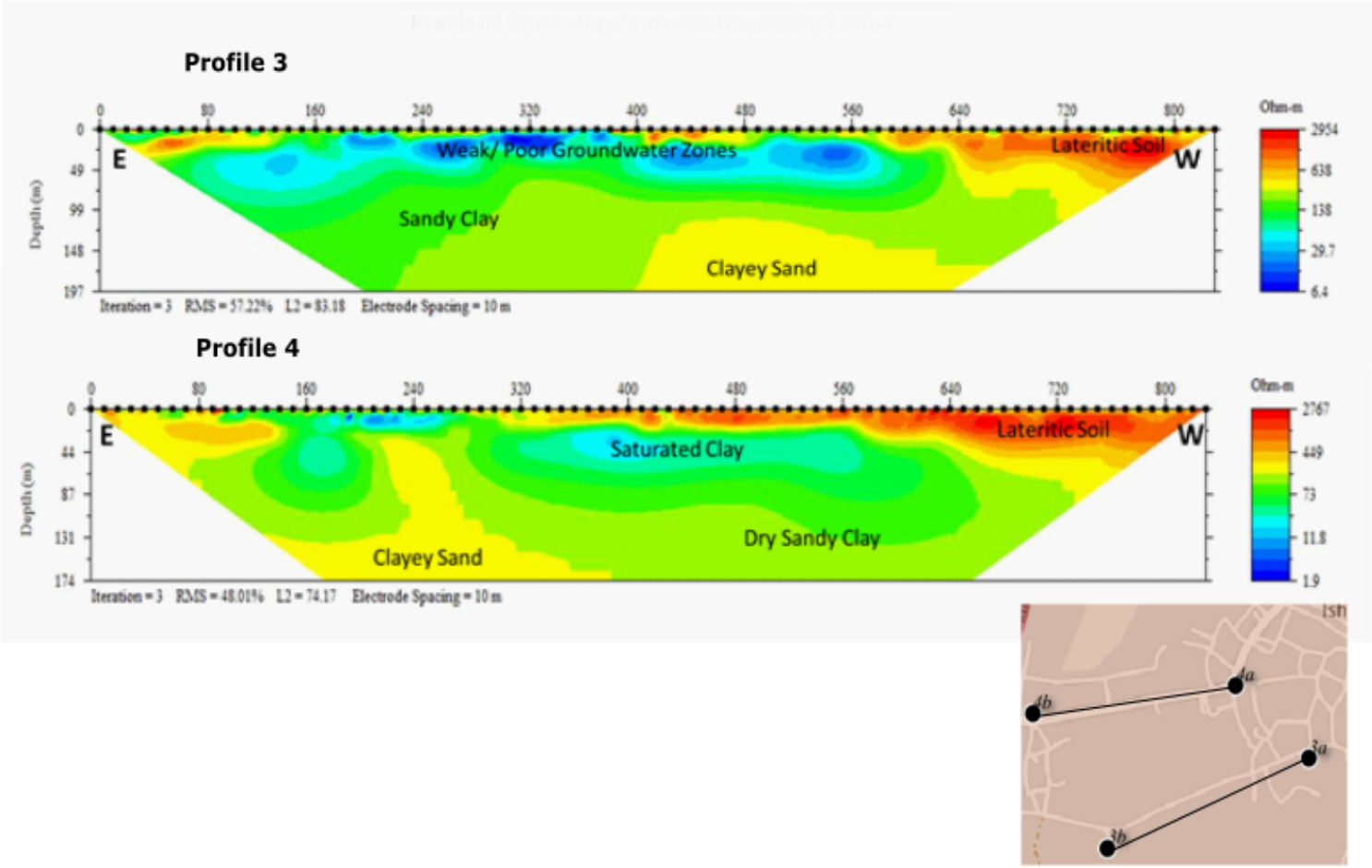

Figure 4

Dipole dipole inverted resistivity sections across Profile 3 and 4 in Ward 2

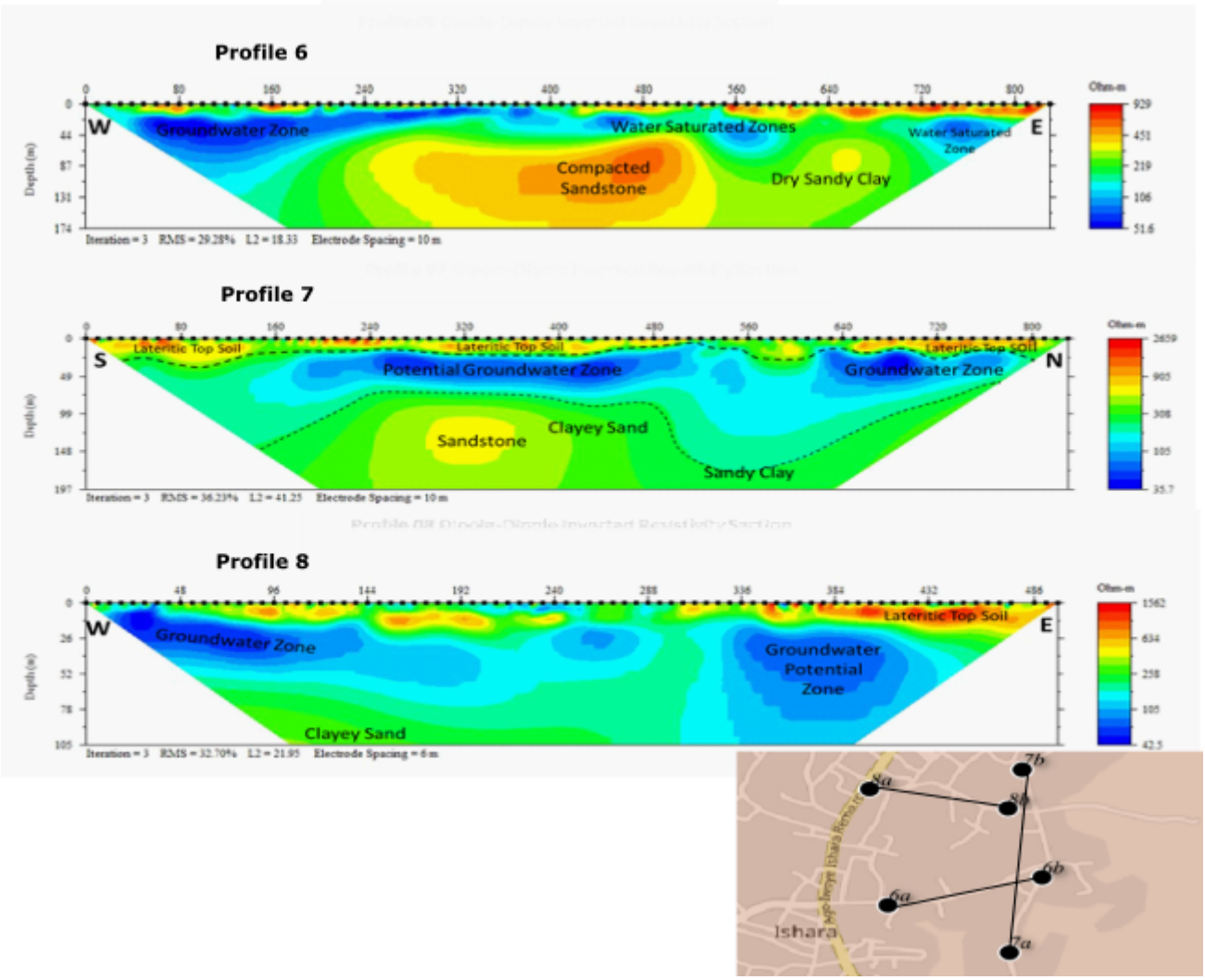

Figure 5

Dipole-dipole inverted resistivity sections across Profile 6, 7 and 8 in Ward 3

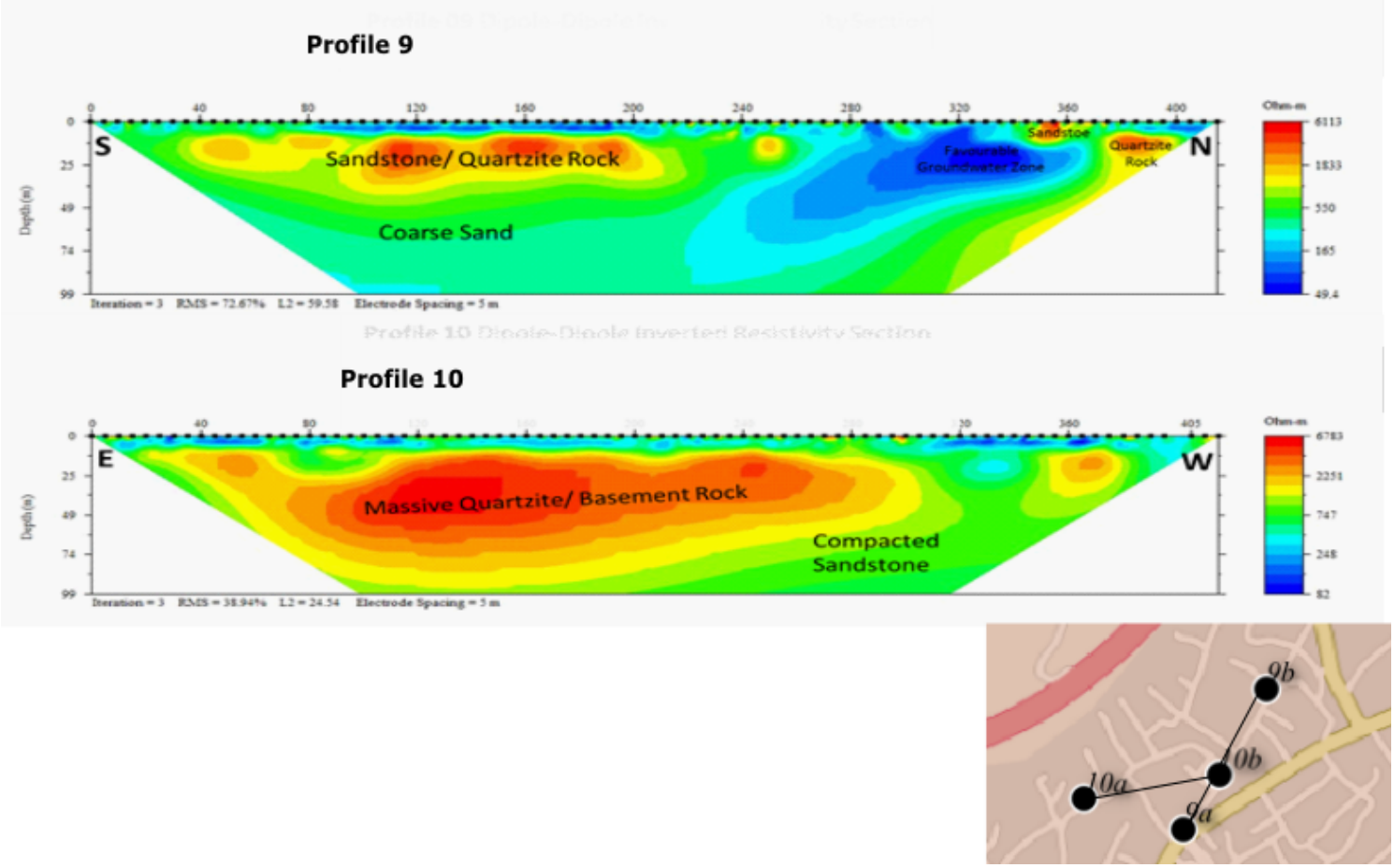

Figure 6

Dipole-dipole inverted resistivity sections across Profile 9 and 10 in Ward 4